Vibrational modes in $Zn_{1-x}Fe_xSe$ and $Zn_{1-x}Co_xSe$

Chee-Leung Mak and R. Sooryakumar
Department of Physics, The Ohio State University, Columbus, Ohio 43210

B. T. Jonker and G. A. Prinz
Naval Research Laboratory, Washington, D.C. 20375
(Received 8 August 1991)

We report on a Raman study of lattice vibrations in the diluted magnetic semiconductors $Zn_{1-x}Fe_xSe$ ($0<x<0.64$) and $Zn_{1-x}Co_xSe$ ($0<x<0.10$). Both alloys possess a homogeneous crystal phase having the zinc-blende structure. The observed dependence of the first-order optical-phonon spectrum on x follows the mixed-mode behavior and is well described by the modified random-element isodisplacement model. Several physical parameters for the end members, cubic FeSe and CoSe, are deduced from the fits to the composition dependence of the lattice vibrations.

I. INTRODUCTION

The vibrational spectra of tertiary mixed crystals are known to vary between the two extreme limits of one-mode and two-mode behavior. While there have been several treatments to account for the phonon properties of mixed crystals, it remains difficult to predict *a priori* the nature of the vibrations in a given alloy. The particular characteristics of such behavior are often determined by the vibrational properties of the binary end components. Thus the phonon spectrum of the alloy can be utilized to predict specific macroscopic characteristics of end members that may not be readily stabilized in a particular lattice structure.

In addition to the vibrational modes in the III-V based mixed crystals, phonons in diluted-magnetic-semiconductor (DMS) alloys with manganese as a dopant have been studied in recent years.[1] Among the latter the phonon spectra of $Cd_{1-x}Mn_xTe$,[2] $Zn_{1-x}Mn_xTe$,[3,4] and $Zn_{1-x}Mn_xSe$ (Ref. 5) have been investigated in considerable detail. In this paper we probe the optical-phonon-mode behavior of $Zn_{1-x}Fe_xSe$ and $Zn_{1-x}Co_xSe$, a recent class of DMS's, and interpret our results using the modified random-element isodisplacement (MREI) model.[6]

According to this model, three distinct mode types can be expected in alloys: namely one-, two-, and mixed-mode behavior. In the one-mode case, the zone-center optical-phonon frequencies vary continuously with concentration within the frequencies of the two end members. In two-mode behavior, each TO-LO phonon pair for an end member degenerates to an impurity mode of the other end member. Between these limits lies the mixed-mode, which shows intermediate behavior. Raman scattering from the DMS $Cd_{1-x}Mn_xTe$ (Ref. 2) showed that it exhibits two-mode behavior. Since the masses of Zn and Mn are more closely matched than Cd and Mn, it was expected that the Zn-Mn DMS would be qualitatively different from its Cd-based counterpart. Both $Zn_{1-x}Mn_xTe$ and $Zn_{1-x}Mn_xSe$ were shown[3-5] to behave as mixed-mode systems. Based upon their relative masses, the vibrational properties of $Zn_{1-x}Fe_xSe$ and $Zn_{1-x}Co_xSe$ are expected to be similar to $Zn_{1-x}Mn_xSe$. This is confirmed in our study. Interpretation of our results within the MREI framework provides for an estimate of the phonon frequencies and dielectric constants of the end members cubic FeSe and CoSe.

II. EXPERIMENTAL DETAILS

The $Zn_{1-x}Fe_xSe$ and $Zn_{1-x}Co_xSe$ samples used in our study were single-crystal epilayers grown by molecular-beam epitaxy on (001) GaAs substrates. Details of the growth conditions have been published elsewhere.[7] The epilayer thickness ranged from 0.25 to 1.56 μm, and the film was oriented with the [001] direction (z axis) oriented normal to the surface. The Raman spectra at room temperature were excited using the 457.5-, 488-, and 514.5-nm lines of an Ar^+-ion laser with a power of about 200 mW. The backscattered light was analyzed with a Spex double-grating monochromator and detected using standard single-channel photon-counting techniques.

III. RESULTS

Polarized Raman spectra in the vicinity of the optical-phonon frequencies for $Zn_{1-x}Fe_xSe$ ($x=0$, 0.027, 0.088 , and 0.22) and $Zn_{1-x}Co_xSe$ ($x=0.0076$, 0.037 and 0.094) are shown in Figs. 1 and 2. The standard notation has been utilized, where $z(x,y)\bar{z}$ denotes the incoming radiation along $z(\|[001])$ being polarized along $x(\|[100])$ with the backscattered ($\bar{z}$) light polarized along $y(\|[010])$. In Fig. 1 the spectrum of pure ZnSe consists of a longitudinal-optical phonon LO_1 (253 cm^{-1}) and weak leakage from the transverse mode TO_2 (204 cm^{-1}). The peaks at 270 and 292 cm^{-1} (identified with asterisks) are, respectively, the transverse- and longitudinal-optical phonons of the GaAs substrate. There is a second-order zone-boundary $2TA(X)$ mode, at $\omega_1=140$ cm^{-1} in Fig. 1. The location of this two-phonon

feature is in agreement with a peak in the density of states at 70 cm^{-1} associated with an X-point acoustic-phonon vibration. We observe that the LO_1-TO_2 pair and 2TA(X) mode occur at about the same frequencies in $Zn_{1-x}Fe_xSe$ ($x=0.027$) as those in ZnSe. At this concentration and beyond, an additional Raman peak, labeled B, with A_1 symmetry develops. The frequency of this Raman peak ($\omega_2=161$ cm^{-1}) is independent of composition, and its intensity is, relative to other phonon features, independent of temperature. This eliminates the assignment of peak B to a difference mode, as, for example, a LO-TA(L) mode. The intensity of this impurity-related mode also increases with x. We assign this A_1 mode to a disorder-induced breathing mode of the near-neighbor Se ions around an impurity atom which remains immobile. In such a case, the mode frequency would not depend on the mass of the impurity atom, but is determined solely by its interactions with the nearest-neighbor Se atoms. A similar feature has also been reported in $Zn_{1-x}Mn_xTe$ (Ref. 4) and $Cd_{1-x}Mn_xTe$.[2] Besides these modes there is an additional peak at 230 cm^{-1}, labeled LO_2 and lying between the zone-center transverse and longitudinal vibrations of the host. This mode, which is first evident at $x=2.7\%$, has the same symmetry as LO_1 and becomes more distinct and shifts to lower frequency as x increases. With decreasing temperature the frequency of LO_2 increased at the same rate as the LO_1 mode. Based on our discussions below, LO_2 is identified as the band mode ZnSe:Fe in the mixed crystal.

We now turn to $Zn_{1-x}Co_xSe$ whose phonon spectra are similar to $Zn_{1-x}Fe_xSe$. From Fig. 2 we observe, as in $Zn_{1-x}Fe_xSe$, that the frequency of the LO_1 mode har-

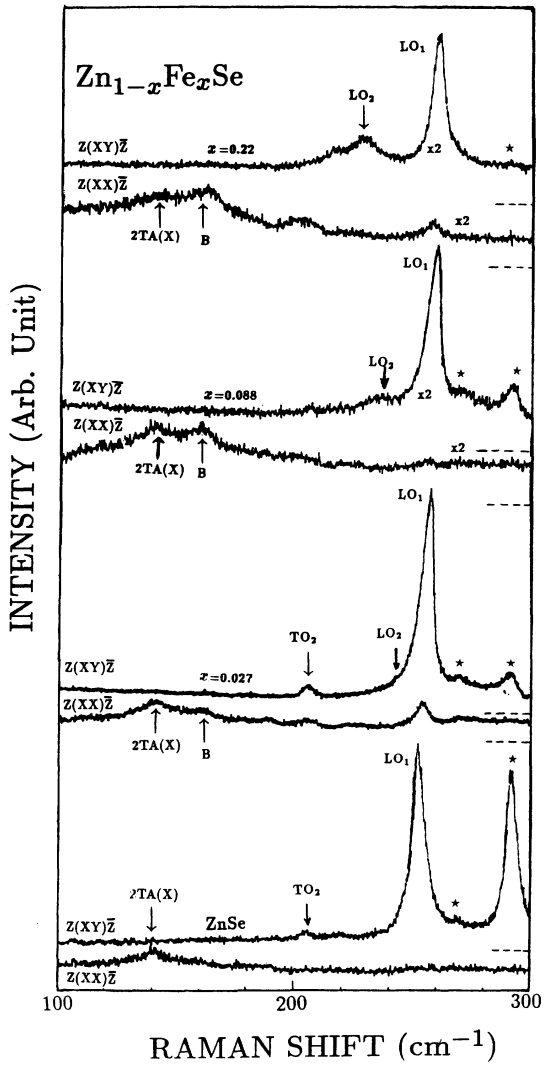

FIG. 1. Room-temperature Raman spectra for $Zn_{1-x}Fe_xSe$ excited at $\lambda=514.5$ nm ($x=0.088$ and ZnSe) and $\lambda=488$ nm ($x=0.027$ and 0.22) in depolarized and polarized backscattering geometries. The two spectra for each sample have been displaced for clarity, with the dashed line indicating the zero reference.

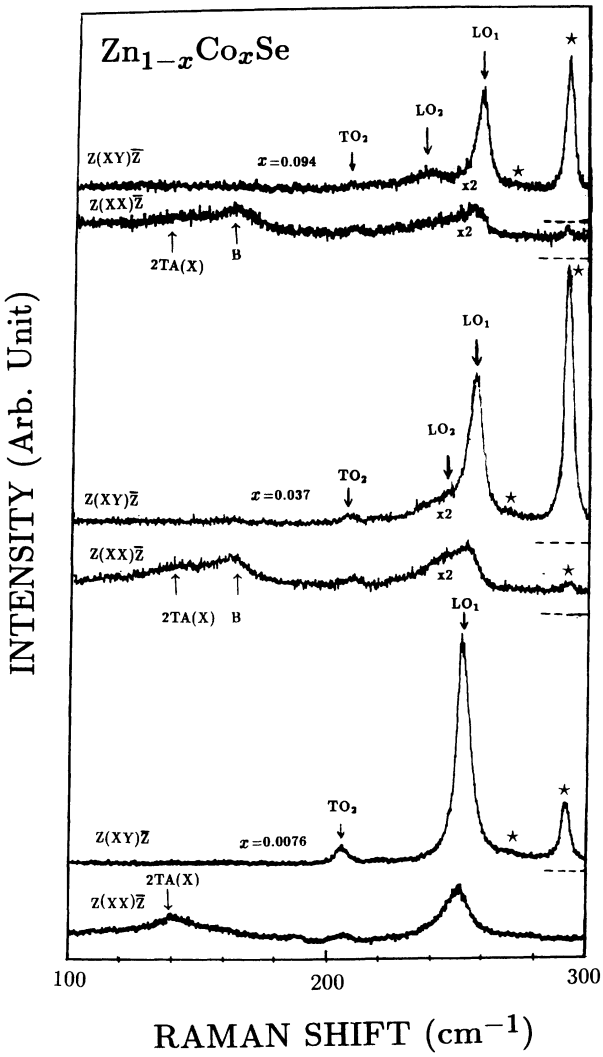

FIG. 2. Room-temperature Raman spectra for $Zn_{1-x}Co_xSe$ ($x=0.0076$, 0.037, and 0.094) excited at $\lambda=488$ nm in depolarized and polarized backscattering geometries. The two spectra for each sample have been displaced for clarity, with the dashed line indicating the zero reference.

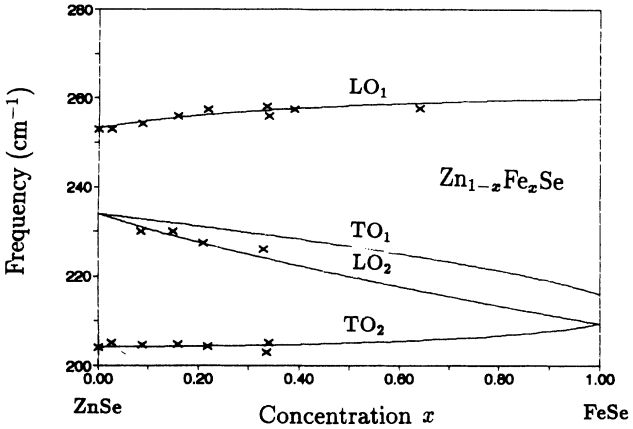

FIG. 3. Frequencies of zone-center optical phonons in $Zn_{1-x}Fe_xSe$ at room temperature. The crosses are the measured frequencies, while the curves were generated using the MREI model described in the text. The data were obtained from Raman spectra excited at 514.5, 488, and 457.5 nm.

dens with increasing x up to 0.10. The second-order phonon 2TA(X) mode is also observed in polarized scattering. For $x > 0.76\%$, peak B of A_1 symmetry (160 cm^{-1}) lying at a frequency very close to the breathing mode in $Zn_{1-x}Fe_xSe$ begins to emerge. This mode displays a similar behavior as the corresponding excitation in $Zn_{1-x}Fe_xSe$, i.e., composition-independent frequency and temperature-independent intensity. We thus assign this feature to the breathing mode in $Zn_{1-x}Co_xSe$. Similar to the spectra in Fig. 1, a band-mode LO_2 around 235 cm^{-1} is observed in $Zn_{1-x}Co_xSe$.

Leakage of the longitudinal phonon LO_1 in polarized scattering $[z(xx)\bar{z}]$ is visible from Figs. 1 and 2 in both $Zn_{1-x}Fe_xSe$ and $Zn_{1-x}Co_xSe$. This disorder-induced breakdown of the selection rules is especially evident when excited at 488 nm, which is in near resonance with the energy gap of the host. It is noted that the LO_1 peak

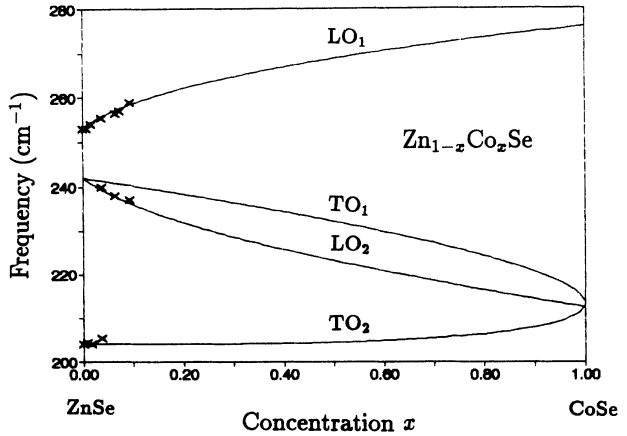

FIG. 4. Frequencies of zone-center optical phonons in $Zn_{1-x}Co_xSe$ at room temperature. The crosses are the measured frequencies, while the curves were generated using the MREI model described in the text. The data were obtained from Raman spectra excited at 514.5, 488, and 457.5 nm.

observed in A_1 symmetry in $Zn_{1-x}Co_xSe$ displays an asymmetric line shape, and preliminary results of this behavior have been discussed elsewhere.[8]

Figures 3 and 4 summarize our results and show the optical-phonon frequencies in $Zn_{1-x}Fe_xSe$ and $Zn_{1-x}Co_xSe$ as a function of dopant concentration x. The crosses correspond to the zone-center optical phonons. The solid curves, as discussed below, are fits to the data based on the MREI model.[6]

IV. DISCUSSION

In this model the mixed crystal $AB_{1-x}C_x$ is assumed to consist of two sublattices, one composed of only A atoms, while the second has a random distribution of B and C. The statistical average of the neighbors depends on the concentration x. The main assumption underlying the isodisplacement model is that, in the long-wavelength limit, the cations and anions of like species vibrate with a single phase and amplitude. Following Ref. 4, where second-neighbor interaction forces F_s were considered, three equations of motion for atoms A, B, and C can be expressed in terms of the force constant f, which is taken to vary linearly with x, i.e.,

$$f(x)=F\{1+\theta[a_c-a(x)]/a_c\}\ .$$

a_c is the lattice parameter of the end member AC (cubic FeSe/CoSe), $a(x)$ the lattice constant of the alloy at concentration x, and F and θ are constants. Since $a(x)$ has been measured[7] and found to vary linearly with x for the dopant concentrations utilized in this study, a_c was estimated through linear extrapolation. The constant F is determined from the optical-phonon frequencies as $x \rightarrow 1$.

The microscopic parameters appearing in the equations of motion can be related,[6] with the aid of Born-Huang relations,[9] to macroscopic quantities such as the static and high-frequency dielectric constant and zone-center phonon frequencies of the binary crystals AB and AC. Since in our case the crystal AC, cubic FeSe, or CoSe, does not exist, we utilize the static dielectric constant $\epsilon_{0(AC)}$, high-frequency dielectric constant $\epsilon_{\infty(AC)}$, and TO frequency $\omega_{TO(AC)}$, together with the constant θ as fitting parameters.

Following the arguments of Peterson *et al.*,[4] the MREI model based eigenfrequencies in $Zn_{1-x}Fe_xSe$ and $Zn_{1-x}Co_xSe$ are given by expressions similar to Eq. (10) of Ref. 4. Table I summarizes the corresponding parameters that provided the best fit to our data. In obtaining the solid curves in Fig. 3, different fitting parameters were found to affect segments of the dispersion to varying degrees. For example, θ largely determined the curvature of the curve labeled LO_1 in Figs. 3 and 4, while the gap mode FeSe:Zn (CoSe:Zn), occurring below the frequency TO_1 as $x \rightarrow 1$, softened with increasing θ. As expected, the dispersion over the whole range of x was more sensitive to the ratio $\epsilon_{0(AC)}/\epsilon_{\infty(AC)}$, rather than to the individual dielectric constants of the end member AC. This accounts for the larger uncertainties placed on the individual parameters $\epsilon_{0(AC)}$ and $\epsilon_{\infty(AC)}$. The nearest-neighbor force constants F_{AC},F_{AB} and the

TABLE I. Parameters in the MREI model.

$Zn_{1-x}Fe_xSe$	Experimental	$Zn_{1-x}Co_xSe$
$\Omega_{I(ZnSe:Fe)}=234\ cm^{-1}$		$\Omega_{I(ZnSe:Co)}=242\ cm^{-1}$
$a(x)=5.668+0.091x$ Å (Ref. 7)		$a(x)=5.668+0.058x$ Å (Ref. 7)
	$\Omega_{TO(ZnSe)}=204\ cm^{-1}$	
	$\Omega_{LO(ZnSe)}=253\ cm^{-1}$	
	$\epsilon_{0(ZnSe)}=8.8$ (Ref. 15)	
	Fitting parameters	
FeSe		CoSe
$\epsilon_0=10\pm4$		$\epsilon_0=11\pm4$
$\epsilon_\infty=7\pm2$		$\epsilon_\infty=6\pm2$
$\epsilon_0/\epsilon_\infty=1.47\pm0.05$		$\epsilon_0/\epsilon_\infty=1.66\pm0.05$
$\Omega_{TO}=216\pm2\ cm^{-1}$		$\Omega_{TO}=214\pm2\ cm^{-1}$
$\theta=3\pm1$		$\theta=4\pm2$
	Resultant force constants	
$F_{AB}:F_{Zn\text{-}Se}=1.99\times10^6$ amu (cm^{-2})		
$F_{AC}:F_{Fe\text{-}Se}=2.07\times10^6$ amu (cm^{-2})		
$F_{AC}:F_{Co\text{-}Se}=2.32\times10^6$ amu (cm^{-2})		
$F_s:F_{Zn\text{-}Fe}=8.73\times10^5$ amu (cm^{-2})		
$F_s:F_{Zn\text{-}Co}=9.66\times10^5$ amu (cm^{-2})		

second-neighbor constant F_s were largely determined by the frequencies of the gap mode and transverse-optical phonon of the lattice as $x\rightarrow1$ and of the host ZnSe.

As seen from Figs. 3 and 4, the curves generated from this MREI model fit the experimental results well. The magnitude of the second-neighbor force constant F_s ($F_{Zn\text{-}Fe}$, $F_{Zn\text{-}Co}$) ranges from one-half to one-third that of the nearest-neighbor constants F_{AB} ($F_{Zn\text{-}Se}$) and F_{AC} ($F_{Fe\text{-}Se}$, $F_{Co\text{-}Se}$), which is reasonable. The vibrational modes that evolve from ZnSe are designated as LO_1 and TO_2. As x increases, the band mode splits into the longitudinal mode LO_2 and transverse TO_1 mode at a higher frequency. For the scattering geometry conveniently available, mode TO_1 is forbidden and hence not observed. Moreover, as the Fe concentration increases, the mixed crystal becomes more metallic, rendering the allowed phonon peaks to be weak. As a result, only the strongest peak LO_1 was observed in $Zn_{0.36}Fe_{0.64}Se$ when excited at 457.5 nm. As $x\rightarrow1$, the LO_1 mode of the host ZnSe has evolved into the LO mode of FeSe (CoSe), while the TO_1 phonon emerging from the band mode ZnSe:Fe (ZnSe:Co) approaches the TO vibration of the hypothetical zinc-blende FeSe (CoSe) lattice. Phonons TO_2 and LO_2 merge to become the gap mode FeSe:Zn (CoSe:Zn), lying at 209 cm^{-1} (213 cm^{-1}) between the zone-edge acoustic and optic modes of the lattice AC.

From Figs. 3 and 4, the TO-LO phonon pair of ZnSe and the band mode ZnSe:Fe (ZnSe:Co) lying at a frequency of 234 cm^{-1} (242 cm^{-1}) between the LO and TO modes of the host are evident as $x\rightarrow0$. The existence of a local mode lying above the TO phonon of ZnSe:Fe(CO) is in agreement with predictions of Lucovsky, Brodsky, and Burstein[10] who have investigated local mode frequencies in diatomic systems. Eigenfrequencies of these impurity-related modes thus estimated occur at 225 and 223 cm^{-1} and are close to the measured values in the Fe- and Co-doped films.

To analyze the mode behavior, we use the result of Chang and Mitra.[11] Their criteria only assumes the existence of one- and two-mode behavior and does not predict whether the alloy will display mixed-mode characteristics. If, as in $Zn_{1-x}Fe_xSe$ and $Zn_{1-x}Co_xSe$, the masses of the substituting elements are greater than the reduced masses of the mixing compounds; i.e., if both $m_B>\mu_{AC}$ and $m_C>\mu_{AB}$, then the crystal is expected to be a one-mode system. Otherwise, it should feature two-mode traits. On combining this result with the frequency of the impurity vibration, which has been placed as a band mode in ZnSe:Fe and ZnSe:Co and evolves to a gap mode as $x\rightarrow1$, it is seen that the Fe- and Co-based DMS's are not described by one-mode behavior. Thus, since the system also does not support a two-mode behavior, we conclude that $Zn_{1-x}Fe_xSe$ and $Zn_{1-x}Co_xSe$ should, as observed, display mixed-mode characteristics.

We also consider predictions on the mode behavior based on a much simpler rule.[12] A mixed system $AB_{1-x}C_x$ should exhibit (a) one-mode behavior if $m_A<m_B,m_C$, (b) mixed-mode behavior if $m_B<m_A<m_C$, and (c) two-mode behavior is $m_A>m_B,m_C$. Following these rules, in both Fe- and Co-substituted ZnSe, case (c) is satisfied, which should give us, contrary to measurement, two-mode behavior. We thus see, in agreement with other observations,[13] that, while the sulfide system appears to follow this simpler rule, the Se-based

structures do not.

Finally, we note that on applying the results of Ref. 10 to the DMS $Zn_{1-x}Ni_xSe$, we predict a band mode for ZnSe:Ni at 223 cm^{-1} and a gap mode at the other end NiSe:Zn. Based on the trend from MnSe:Zn, FeSe:Zn to CoSe:Zn, the frequency difference between the TO phonon and gap modes becomes smaller (differences 20,[5] 7, and 1 cm^{-1}, respectively), and we expect the NiSe:Zn gap mode to lie very close to the TO phonon in cubic NiSe. Moreover, since $m_{Zn}=65.4>\mu_{NiSe}=33.7$ and $m_{Ni}=58.7>\mu_{ZnSe}=35.8$, based on the arguments utilized above for Co- and Fe-based mixed crystals, we expect the Ni alloy to also display mixed-mode behavior. Our measurements on such nickel-doped films with x up to 3.2%, however, did not reveal evidence of the band mode ZnSe:Ni. While these low concentrations may be inadequate to detect the emergence of dopant-induced phonon effects, attempts to incorporate higher x values within the lattice were difficult as a result of phase separation.

V. CONCLUSIONS

The optical phonons of $Zn_{1-x}Fe_xSe$, $0\le x\le 0.22$, and $Zn_{1-x}Co_xSe$, $0\le x\le 0.094$, display a behavior that is intermediate to the one- and two-mode cases and similar to that reported in $Zn_{1-x}Mn_xSe$. Although CoSe and FeSe have yet to be stabilized in the zinc-blende structure,[14] some of their physical characteristics have been deduced from the study of alloys for which it constitutes an end member.

ACKNOWLEDGMENTS

This work was supported at The Ohio State University by the National Science Foundation under Grant No. DMR-90 0167 and at NRL by the Office of Naval Research.

[1]For a review see *Diluted Magnetic Semiconductors,* edited by J. K. Furdyna and J. Kossut, Vol. 25 of *Semiconductors and Semimetals,* edited by R. K. Willardson and A. C. Beer (Academic, San Diego, 1988).

[2]S. Venugopalan, A. Petrou, R. R. Galazka, and A. K. Ramdas, Phys. Rev. B **25**, 2681 (1982).

[3]B. Oles and H. G. Schering, J. Phys. C **18**, 6289 (1985).

[4]D. L. Peterson, A. Petrou, W. Giriat, A. K. Ramdas, and S. Rodriguez, Phys. Rev. B **33**, 1160 (1986).

[5]A. K. Arora, E. K. Suh, U. Debska, and A. K. Ramdas, Phys. Rev. B **37**, 2927 (1988).

[6]L. Genzel, T. P. Martin, and C. H. Perry, Phys. Status Solidi B **62**, 83 (1974).

[7]B. T. Jonker, J. J. Krebs, and G. A. Prinz, Appl. Phys. Lett. **53**, 450 (1988); B. T. Jonker, J. J. Krebs, S. B. Qadri, and G. A. Prinz, *ibid.* **50**, 848 (1987).

[8]C. L. Mak, R. Sooryakumar, B. T. Jonker, and G. A. Prinz, in *Proceedings of the 20th International Conference on The Physics of Semiconductors,* edited by E. Anastassakis and J. Joannopoulos (World Scientific, Singapore, 1990), p. 1815.

[9]M. Born and K. Huang, *Dynamical Theory of Crystal Lattices* (Oxford University Press, London, 1968).

[10]G. Lucovsky, M. H. Brodsky, and E. Burstein, Phys. Rev. B **2**, 3295 (1970).

[11]I. F. Chang and S. S. Mitra, Phys. Rev. **172**, 924 (1968).

[12]L. Genzel and W. Bauhofer, Z. Phys. B **25**, 13 (1976).

[13]A. Anaslassiadou, E. Liarokapis, and E. Anastassakis, Solid State Commun. **69**, 137 (1989).

[14]Thick FeSe films (> 500 Å) exhibit a tetragonal structure. Thinner films have not been sufficiently characterized to date. See B. T. Jonker, J. J. Krebs, G. A. Prinz, X. Liu, A. Petrou, and L. Salamanca-Young, in *Growth, Characterization and Properties of Ultrathin Magnetic Films and Multilayers,* edited by B. T. Jonker, E. E. Marinero, and J. P. Heremans, MRS Symposium Proceedings No. 151 (Materials Research Society, Pittsburgh, 1989), p. 151; S. B. Qadri, B. T. Jonker, J. J. Krebs, and G. A. Prinz, Thin Solid Films **164**, 111 (1988).

[15]*Numerical Data and Functional Relationships in Science and Technology,* edited by O. Madelung (Springer-Verlag, Heidelberg, 1982), Vol. 17b, Sec. 3.7, p. 149.